EXPERIMENTAL INVESTIGATION OF COLLISIONLESS SHOCK WAVES IN A PLASMA

A. M. ISKOL'DSKIĬ, R. Kh. KURTMULLAEV, Yu. E. NESTERIKHIN, and A. G. PONOMARENKO

Nuclear Physics Institute, Siberian Division, Academy of Sciences, U.S.S.R.

Submitted to JETP editor May 9, 1964

J. Exptl. Theoret. Phys. (U.S.S.R.) **47**, 774-776 (August, 1964)

A number of authors[1-4] have discussed the possibility of propagation of shock waves with fronts considerably thinner than the mean free path in a rarefied plasma. It has been suggested that this mechanism is responsible for the propagation of strong hydromagnetic perturbations generated by solar flares in the interplanetary plasma. Preliminary estimates of the front thickness for the perturbations were made by Moiseev and Sagdeev[5] on the basis of rocket measurements.[6] An attempt to observe this effect in a laboratory plasma was made by Patrick.[7] Later, however, Patrick concluded that it is impossible to relate these observations to collisionless plasma dynamics because under the conditions of his experiment ($n > 10^{15}$ cm^{-3}, where n is the ion density, approximately of the same order as the neutral density) the mean free path for charge exchange is smaller than, or equal to, the thickness of the observed wave front.

We present below the preliminary results of an investigation of shock wave propagation in a plasma of considerably lower density ($n < 10^{14}$ cm^{-3}), for which the mean free path for charge exchange is much greater than the path traversed by the shock wave.

A diagram of the experimental arrangement is shown in Fig. 1. A glass tube 166 mm in diameter and 2500 mm in length is located in an axial magnetic field $H_0 \sim 2000$ Oe; a pre-ionized plasma whose density is monitored by microwaves is produced in the tube. When the plasma occupies the volume under the turn 3, a low-inductance capacitor bank is discharged through this turn so that a rapidly rising magnetic field is produced at the edge of the plasma (the characteristic rise time is 0.2×10^{-6} sec); the field amplitude is $(2-3)\,H_0$. The behavior of the converging cylindrical hydromagnetic perturbation generated by this "magnetic piston" was investigated by means of an electron-optical image converter (EIC). The pictures were taken through a transverse slit in the turn (cf. Fig. 1).

In Fig. 2a we show a time-swept photograph of the emission from the shock wave in a helium plasma ($n \sim 3 \times 10^{13}$ cm^{-3}, $H_0 \approx 10^3$ Oe). On the sawtooth sweep voltage is superimposed a sinusoidal low-amplitude calibration signal (period 0.03×10^{-6} sec). The photograph shows the front of a converging wave moving toward the center with a velocity 4×10^7 cm/sec. Microphotometry of the films with an MF-4 instrument has made it possible to detect some increase in the intensity

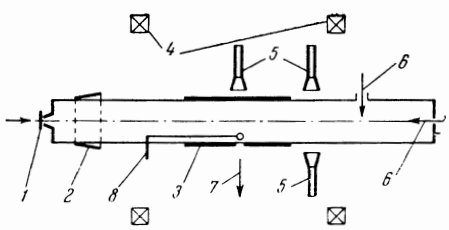

FIG. 1. 1) Electrodynamic pulsed neutral gas input, 2) conical coil that produces the preionized plasma, 3) shock coil that produces the magnetic piston, 4) coils that produce the primary axial magnetic field, 5) microwave horns (used to measure plasma density and microwave noise), 6) scintillation counter for fast electrons and x rays, 7) transverse slit for image-converter observation of the shock wave, 8) magnetic probes, 1 mm.

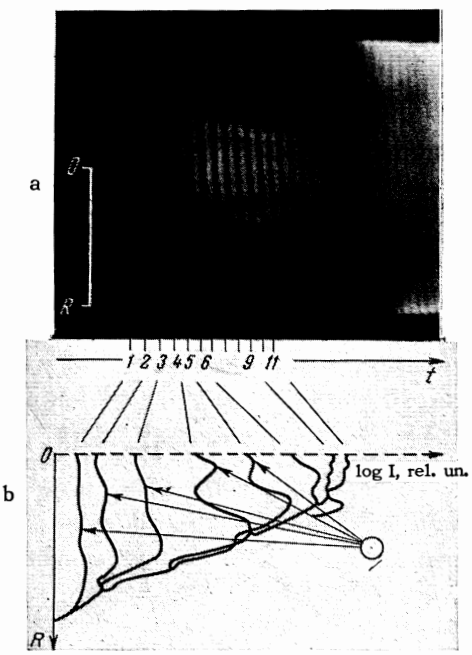

FIG. 2. a) Shock wave in a helium plasma. The vertical bands occur every 0.03 μsec; b) results of microphotometry of the image in the radial direction. The arrows indicate oscillations which arrive before the main front. The curves refer to times denoted in Fig. 2a by the numbers and characterize the time behavior of the process. Along the abcissa axis is plotted the logarithm of the emission intensity in relative units.

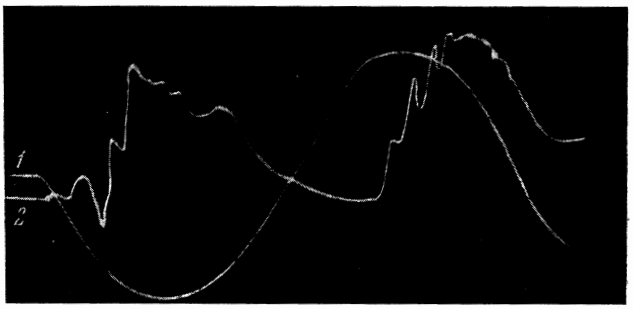

FIG. 3. 1) Oscillogram showing the current in the shock circuit with a period $1.4 \cdot 10^{-6}$ sec, 2) oscillogram showing the variation of magnetic probe located at a distance of 8 mm from the chamber axis. The oscillatory nature of the shock fronts produced in the first and second half cycles of the current is evident.

of the light ahead of the main front; this could be identified as an additional oscillation that propagates ahead of the main front (cf. Fig. 2b). Microphotograms of the images obtained at later times can be used to estimate the propagation velocity of this perturbation (4.6×10^7 cm/sec).

Using similar apparatus, we have carried out experiments to examine the structure of the magnetic field within the shock front of the hydromagnetic perturbation, using magnetic probes.

In Fig. 3 we show a typical oscillogram of the shock front of a magnetic perturbation ($n \sim 4 \times 10^{13}$ cm^{-3}, $H_0 \sim 300$ Oe) obtained with a magnetic probe (diameter 0.8 mm) located at a distance of 8 mm from the axis of the chamber. The photograph shows the delay in the arrival of shock, due to its finite propagation velocity, and also shows the variation of the magnetic field ahead of the main wave (oscillation). Thus, the image-converter measurements described above and the magnetic-probe measurements point to the existence of oscillations within the front of a collisionless shock. The results of these preliminary experiments provide qualitative verification of the oscillatory front structure predicted by the theory.[8,9] Thus in the case of a wave propagating at an angle φ of approximately $\pi/2$ to the direction of the initial magnetic field ($1 \gg \pi/2 - \varphi > \sqrt{m/M}$ where m and M are respectively the electron and ion masses), the theory predicts that the spatial scale length of the oscillations leading the main front should be of order $c\theta/\Omega_0$ where $\Omega_0 = (4\pi ne^2/M)^{1/2}$ is the ion plasma frequency and $\theta = |\pi/2 - \varphi|$. For $n \sim 3 \times 10^{13}$ cm^{-3} and a helium plasma agreement can be obtained between the expected scale size of the oscillations $c\theta/\Omega_0$ and the observed values, within the limits of the experimental data acquired so far, provided θ is taken to be the mean angle between the lines of force in the initial magnetic field and the magnetic field produced by the shock turn; this angle is of order $1/10$ and is determined by the ratio of the radius of the turn to its length.

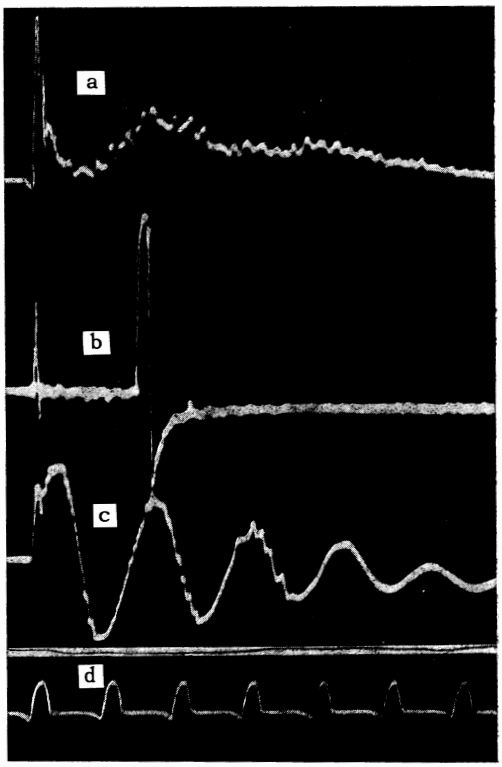

FIG. 4. Radiation from the plasma. a) Signal from the scintillation counter; b) microwave radiation at 0.8 cm, c) current in the shock circuit, d) 1×10^{-6} sec time markers.

In these experiments we have also detected additional effects accompanying the convergence of the shock wave at the axis of the chamber. Thus, at convergence there is a burst of microwave radiation at 3 cm and 0.8 cm (Fig. 4b). Investigations of the spatial distribution of the radiation sources in the 0.8 cm range with highly directive antennas showed that the sources are close to the axis of the system. The microwave radiation was accompanied by a signal in a counter (stilbene covered by a 60μ copper foil) (Fig. 4a). The characteristic lifetime of these signals, $\sim 30 \times 10^{-9}$ sec, corresponds to the transit time of the hydrodynamic perturbation over distance of order 1—2 cm, which correlates with the size of the front estimated by means of the optical and magnetic measurements.

We are presently carrying out systematic investigations of the fine structure of the shock front.

The authors are indebted to G. I. Budker for his continued interest in this work and R. Z. Sagdeev and A. A. Galeev for discussion and help.

[1] R. Z. Sagdeev, Fizika plazmy i problema upravlyaemykh termoyadernykh reaktsiĭ (Plasma Physics and the Problem of a Controlled Thermonuclear Reaction) AN SSSR, 1958, Vol. 4, p. 384; also ZhTF **31**, 1185 (1961), Soviet Phys. Tech. Phys. **6**, 867 (1962).

[2] Gardner et al, Report 374, Conference on the Peaceful Uses of Atomic Energy, Geneva, 1958.

[3] E. Parker, Phys. Rev. **112**, 1429 (1958).

[4] M. Camac et al, Nuclear Fusion, Supp. II, 1963, p. 423.

[5] M. S. Moiseev and R. Z. Sagdeev, J. Nuclear Energy Part C **5**, 43 (1963).

[6] M. Neugebauer and C. W. Snyder, Science **138**, 1095 (1962).

[7] R. Patrick, Phys. Fluids **3**, 321 (1960).

[8] R. Z. Sagdeev, Symposium on Electromagnetics and Fluid Dynamics of Gaseous Plasma, Polytechnic Institute of Brooklyn, 1961. V. I. Karpman, ZhTF **33**, 959 (1963), Soviet Phys. Tech. Phys. **8**, 715 (1964).

[9] R. W. Morton, Finite Amplitude Compression Waves in Collision Free Plasma, AEC Document NYO-10434, New York University, 1964.

Translated by H. Lashinsky
110

THE RELATION BETWEEN THE SCATTERING LENGTH AND THE RADIATIVE CAPTURE CROSS SECTION FOR NEUTRONS

Yu. I. FENIN and F. L. SHAPIRO

Joint Institute for Nuclear Research

Submitted to JETP editor May 15, 1964

J. Exptl. Theoret. Phys. (U.S.S.R.) **47**, 777-778 (August, 1964)

FOR low energy neutrons, when the main contribution to the interaction with nuclei comes from the partial wave for zero angular momentum, there is a simple relation between the cross sections for elastic scattering and for radiative capture of neutrons in the region between resonances:

$$\sigma_{\gamma J}(E) = -g_J \lambda \Gamma_\gamma d a_J(E)/dE. \quad (1)$$

Here $\sigma_{\gamma J}$ is the total cross section for radiative capture of neutrons in the channel with spin J: $g_J = (2J+1)/2(2i+1)$ is the statistical weight for the J channel; i is the spin of the target nucleus; λ is the neutron wave length; Γ_γ is the radiative width; a_J is the amplitude for scattering in the J channel. For even-even nuclei $a_J \equiv a = (\sigma_s/4\pi)^{1/2}$, where σ_s is the scattering cross section. Formula (1) is valid to an accuracy of order $[\Gamma/(E-E_0)]^2 : 1$ and $(kR)^2 : 1$ ($|E-E_0|$ is the distance to the nearest resonance, Γ is the resonance width at energy E, $k = 2\pi/\lambda$ is the wave number of the neutron, and R is the nuclear radius), and is gotten on the following assumptions.

1. There is no interference between resonances in the total cross section for radiative capture. The absence of interference may be regarded as an experimental fact; the reason for the washing out of the interference is the very large number of channels for radiative capture in the case of neutrons of medium or high energy.

2. For resonances with the same spin and parity, the total radiation widths are the same. The experimental data[1] indicate a constant radiation width within the limits of error of the experiments (±10—15%). If the radiation widths are not constant, Γ_γ in (1) will be some average value which has a weak energy dependence.

To obtain (1) we use the expression for the S matrix element which follows from the R matrix theory of Wigner and Eisenbud:[2]

$$S_{st} = e^{-2i\varphi_{st}} \left\{ \delta_{st} + i \sum_\lambda \frac{\Gamma_{\lambda s}^{1/2} \Gamma_{\lambda t}^{1/2}}{E_\lambda - E - i\Gamma_{\lambda\lambda}/2} - \right.$$

$$\left. - \frac{1}{2} \sum_\lambda \sum_{\mu(\neq\lambda)} \frac{\Gamma_{\lambda s}^{1/2} \Gamma_{\mu t}^{1/2} \Gamma_{\lambda\mu}}{(E_\lambda - E - i\Gamma_{\lambda\lambda}/2)(E_\mu - E - i\Gamma_{\mu\mu}/2)} + \ldots \right\}$$

$$\Gamma_{\lambda\mu} = \sum_c \Gamma_{\lambda c}^{1/2} \Gamma_{\mu c}^{1/2}. \quad (2)$$

Here $\Gamma_{\lambda s}$ is the neutron width, $\Gamma_{\lambda t}$ ($t \neq s$) is the partial radiation width, $\varphi_{st} = kR$ for the elastic scattering channel ($t = s$) and is of no importance for the radiative channels ($s \neq t$).

Because of the assumption that there is no interference between resonances in the radiative capture,

$$\sum_{c(\neq s)} \Gamma_{\lambda c}^{1/2} \Gamma_{\mu c}^{1/2} = \Gamma_\gamma \cdot \delta_{\lambda\mu},$$

i.e.,

$$\Gamma_{\lambda\mu} = \Gamma_\gamma \delta_{\lambda\mu} + \Gamma_{\lambda s}^{1/2} \Gamma_{\mu s}^{1/2}. \quad (3)$$

Using (3) and expanding (2) in powers of kR and $\Gamma_\lambda/(E_\lambda - E)$, we get

$$k^2 \sigma_\gamma / \pi = \sum_{t(\neq s)} |S_{st}|^2 = \sum_\lambda \Gamma_{\lambda s} \Gamma_\gamma / (E_\lambda - E)^2 + O[(\Gamma/(E-E_0))^4], \quad (4)$$

$$|a| = |1 - S_{ss}|/2k = \left| R - \sum_\lambda \Gamma_{\lambda s}/2k(E_\lambda - E) \right| \times \{1 + O[(kR + \Gamma/|E-E_0|)^2]\}. \quad (5)$$